Accepted Manuscript

Synthesis and molecular docking of *N* ´-arylidene-5-(4-chlorophenyl)-1-(3,4-dichlorophenyl)-4-methyl-1*H*-pyrazole-3-carbohydrazides as novel hypoglycemic and antioxidant dual agents

Eduardo Hernández-Vázquez, Sandybel Salgado-Barrera, Juan José Ramírez-Espinosa, Samuel Estrada-Soto, Francisco Hernández-Luis

PII: S0968-0896(16)30240-1
DOI: http://dx.doi.org/10.1016/j.bmc.2016.04.007
Reference: BMC 12921

To appear in: *Bioorganic & Medicinal Chemistry*

Received Date: 9 February 2016
Revised Date: 23 March 2016
Accepted Date: 1 April 2016

Please cite this article as: Hernández-Vázquez, E., Salgado-Barrera, S., Ramírez-Espinosa, J.J., Estrada-Soto, S., Hernández-Luis, F., Synthesis and molecular docking of *N* ´-arylidene-5-(4-chlorophenyl)-1-(3,4-dichlorophenyl)-4-methyl-1*H*-pyrazole-3-carbohydrazides as novel hypoglycemic and antioxidant dual agents, *Bioorganic & Medicinal Chemistry* (2016), doi: http://dx.doi.org/10.1016/j.bmc.2016.04.007

Synthesis and molecular docking of *N´*-arylidene-5-(4-chlorophenyl)-1-(3,4-dichlorophenyl)-4-methyl-1*H*-pyrazole-3-carbohydrazides as novel hypoglycemic and antioxidant dual agents

Eduardo Hernández-Vázquez,[a]* Sandybel Salgado-Barrera,[a] Juan José Ramírez-Espinosa,[b] Samuel Estrada-Soto,[b] Francisco Hernández-Luis[a]

a) Facultad de Química, Departamento de Farmacia, Universidad Nacional Autónoma de México, México, DF 04510, México.
b) *Facultad de Farmacia, Universidad Autónoma del Estado de Morelos, Cuernavaca, Morelos 62209, México*

Keywords: diarylpyrazole hybrids, cannabinoid receptor 1, antioxidant capacity, antidiabetic effect, molecular docking

*Corresponding author. Tel: +52 55 56225287, e-mail: eduardo.hervaz@gmail.com

Abstract

Herein, the design and synthesis of ten novel *N´*-arylidene pyrazole-3-carbohydrazides are described. Compounds were pretended to act as dual agents against diabetes and oxidative stress, two correlated pathologies involved in metabolic syndrome development and progression. The antioxidant capacity was evaluated by means of DPPH and FRAP *in vitro* assays. It was found that compounds bearing a hydroxyl group at 4-position of the hydrazone moiety are potent antioxidant entities, being compound **3g** (a syringaldehyde derivative) the most active compound. In addition, the *in vivo* hypoglycemic effect of the analogues was determined. With regard to the above, the cinnamaldehyde derivatives showed a scarce biological activity, while the 4-hydroxy analogues showed the higher glycemia reduction at 7 h after administration. Interestingly, the most potent antioxidants **3b** and **3g** also were of the most active compounds in reducing the plasma glucose, reaching 80 % of reduction in the case of **3g**. Molecular docking binding poses conducted to a plausible interpretation of the biological outcomes and a possible interaction between a hydroxy group and Asn287 of CB1R was proposed as an important feature for enhancing the observed activity.

1. Introduction

Cannabinoid receptor 1 (CB1R) antagonists/inverse agonists are some of the most studied leads directed for the treatment of obesity and metabolic syndrome [1, 2]. Since rimonabant (**1**, Figure 1) was released as a selective CB1R antagonist, there has been an increase in the number of research groups whose efforts focus in the optimization of this kind of molecules [3]. In this sense, 1,5-diarylpyrazole derivatives, such as rimonabant, have a plethora of physiological effects related to food intake control and weight balance [4]. Among the physiological responses mediated by the CB1R blockade, it is noteworthy the metabolic effects in peripheral organs (such as adipose tissue, liver and skeletal muscle), which includes the reduction of adipogenesis, hypoglycemia, thermogenesis, enhancement of lipogenesis, and adiponectin up-regulation [5–8]. The latter effects

not only contribute to weight loss in an independent manner of food intake, but it is also implicated in insulin sensitization and lipid homeostasis. Nonetheless, rimonabant was withdrawn in 2009 due to severe side effects such as depression and suicide [9], though it is still considered as a lead for metabolic disorders treatment.

On the other hand, it is well documented that oxidative stress is a condition implicated in the development and progression of diabetes and its complications [10, 11]. Oxidative stress participates in pathogenesis of diabetes due to their ability to oxidize and damage lipids, DNA and proteins and also by acting as signaling molecules to activate stress-sensitive pathways (i. e. NF-κB, p38 MAPK, SAPK) [12, 13], events that finally produce insulin resistance and β-cell damage [14–16].

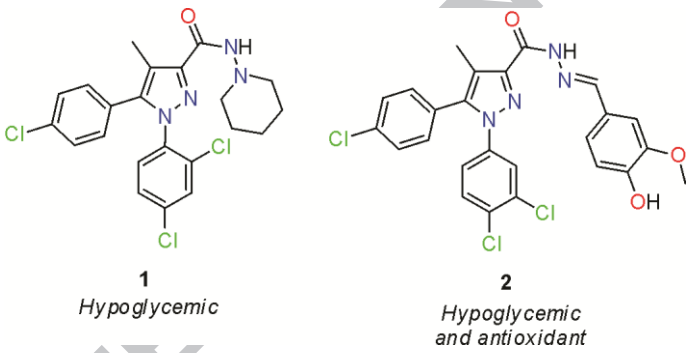

Figure 1. Structures of the pyrazole derivative rimonabant (**1**) and the lead **2**

During our current research concerning the design and synthesis of novel antidiabetic compounds, we found that rimonabant analogues possess an *in vivo* hypoglycemic effect due to its interactions with peripheral CB1R [17]. The latter discovery led us to the synthesis of the 1,5-diarylpyrazole derivative **2** (Figure 1) [18], a dual compound that was demonstrated to exhibit both *in vivo* hypoglycemic and *in vitro* antioxidant activities (in DPPH and ORAC tests). Interestingly, compound **2** bears a vanillinic hydrazone moiety that is responsible for its radical scavenging properties and can be replaced for any other antioxidant portions. Hence, the main goal of this work was the design and preparation of hybrids of compound **2** with several benzaldehyde and cinnamaldehyde derivatives with different oxygenated patterns. Those modifications were selected to verify the

effects in the observed biological effect (both antidiabetic and antioxidant properties) (Figure 2). Additionally, molecular docking studies on a previously modeled CB1R [17] were performed as a computational method to explain the results and also confirm a plausible mechanism of action.

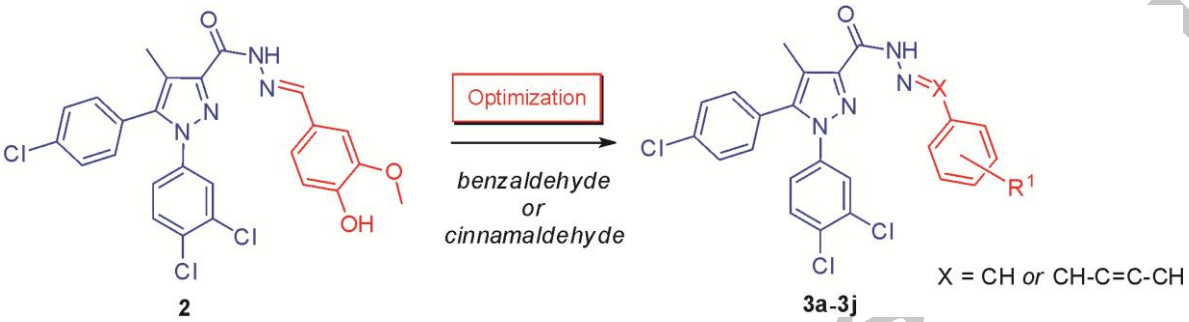

Figure 2. Optimization of compound **2**. R^1 corresponds to different hydroxylated patterns.

2. Results and discussion

2.1. Chemistry

The synthesis of compounds was achieved by following the route showed in Scheme 1. First, 4-chloropropiophenone **4** was treated with LiHMDS in methylcyclohexane and then reacted with diethyl oxalate to obtain the tricarbonylic compound **5**. Afterwards, the condensation of **5** with 3,4-dichlorophenylhydrazine in sulfuric acid and ethanol gave the desired pyrazole ring, which upon a basic hydrolysis provided the pyrazole-3-carboxylic acid **6**. Stirring of **6** in $SOCl_2$/PhMe and the subsequent reaction with *tert*-butyl carbazate, produced the corresponding *N´*-Boc carbohydrazide **7**. Finally, the cleavage of the Boc group with trifluoroacetic acid and the successive condensation with the corresponding aromatic aldehyde generated the hydrazones **3a**–**3j** in good yields. The structures and purity of all compounds was confirmed by spectroscopic (IR and NMR) and spectrometric (mass spectrometry) techniques (See supporting information). Notably, as was previously reported [18], an *E* geometry of the hydrazone double bond is observed and was further corroborated by the NOESY spectrum of compound **3h** and **3j** (Figure S1 and S2 in supporting information). The structure of the diversely decorated *N´*-arylidenehydrazones obtained in this work is shown in Table 1. It is interesting to note that the theoretical pK_i values of compounds **3a**–**3j** (ranging from 7.9 to 8.28) on a highly predictable CoMFA model [7] (Table 1) are in the same

magnitude than rimonabant (experimental pK_i = 7.94 [19]), which demonstrates that compounds would probably have affinity to CB1R and thus a potential hypoglycemic effect.

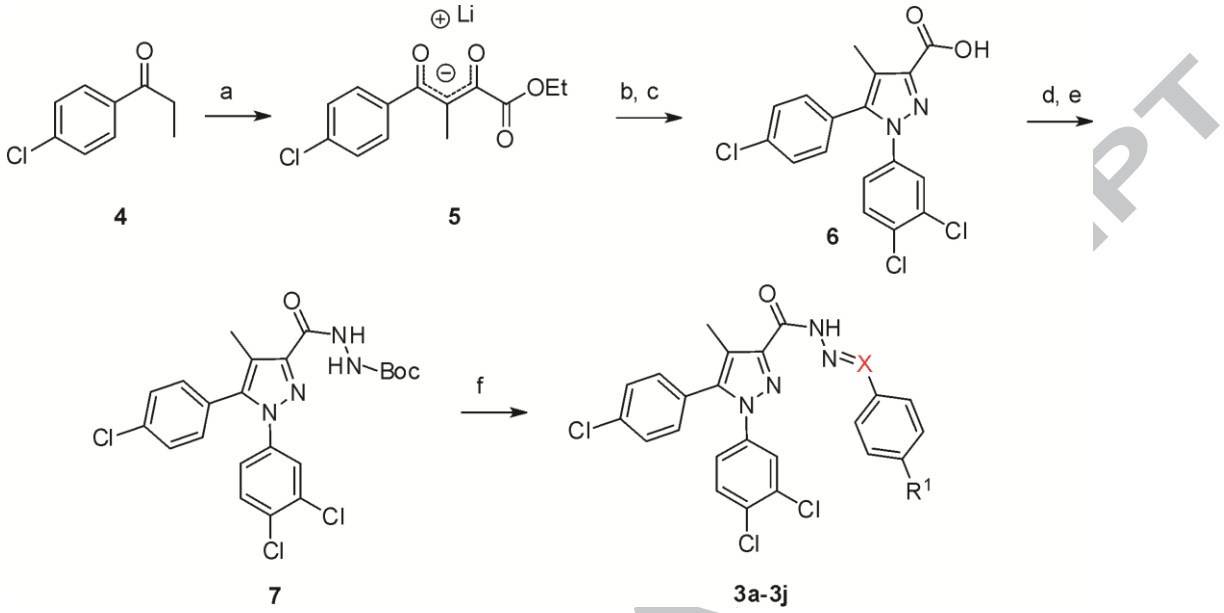

Scheme 1. Synthesis of compounds **3a**–**3j**. Reactions and conditions: (a) LiHMDS, diethyl oxalate, MCH, r.t., 17 h; (b) 3,4-dichlorophenyl hydrazine, EtOH, H_2SO_4, reflux, 8 h; (c) KOH, EtOH, 50 °C, 12 h; (d) $SOCl_2$, PhMe, reflux, 2 h; (e) *tert*-butyl carbazate, DIPEA, $CHCl_3$, 0 °C to r.t., 4 h; (f) TFA, then vanillin, $AcOH_{cat}$, $CHCl_3$, r.t.

Table 1. Structures and DPPH scavenging of *N*'-arylidenehydrazones synthesized in this work

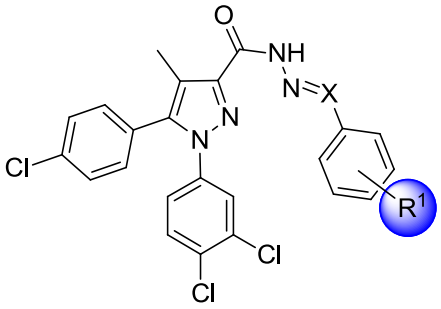

Compound	X	R^1	Yield (%)	Predicted pK_i[a]	% DPPH scavenging			IC_{50}[b] (μM)
					1 μM	10 μM	100 μM	
3a	CH	4-OH	82	8.03	2.76	2.71	6.43	ND
3b	CH	3,4-diOH	83	8.02	9.85	58.60	92.70	10.82 ± 1.55
3c	CH	2,4-diOH	75	8.00	3.57	12.20	22.15	ND
3d	CH	3-OH,4-OMe	78	8.28	1.15	2.46	3.44	ND
3e	CH	3,4-diOMe	73	8.05	2.25	3.73	2.81	ND
3f	CH	3,4-$(OCH_2)_2$	68	7.99	0.72	0.53	1.85	ND
3g	CH	4-OH,3,5-diOMe	54	8.22	11.19	76.24	94.30	8.67±0.25
3h	(*E*)-CH-CH=CH	H	58	8.09	1.58	16.80	90.33	43.41±2.39
3i	(*E*)-CH-CH=CH	4-OH,3-OMe	47	8.15	0.51	12.57	85.33	50.09 ± 1.96
3j	(*E*)-CH-CH=CH	4-OH,3,5-diOMe	61	8.01	1.45	29.39	91.37	32.60 ± 1.52
Ferulic acid	-	-	-	-	3.06	14.52	78.73	47.72 ± 2.31
Sinapic acid	-	-	-	-	2.65	23.29	90.61	35.78 ± 1.74
Quercetin	-	-	-	-	-	-	-	31.74±1.04
α-Tocopherol	-	-	-	-	-	-	-	10.89±0.47

a) Obtained by a CoMFA model [Reference 6]

b) IC_{50} are reported as mean ± standard error (SEM) of n observations (n = 3). ND: not determined.

2.2. Biological activity

Having in hand hydrazones **3a**–**3j**, we proceeded with the biological evaluation of compounds employing both *in vitro* and *in vivo* methods. Since compounds were prepared with the main goal of acting as dual compounds, this section was divided in two principal parts, one concerning to the antioxidant capacity of the analogues and the second related to their potential *in vivo* hypoglycemic effect. The outcomes of these studies are described below.

2.2.1. *In vitro* antioxidant assays

As described previously, there is a narrow relationship between the metabolic syndrome/diabetes and oxidative stress [10, 11]; thus, chemical entities with antioxidant properties are desired in such chronic diseases. According to the latter, derivatives **3a**–**3j** are decorated with different hydroxylated substituents and could exhibit antioxidant effect. Since several antioxidant mechanisms have been attributed to guaiacol derivatives and phenolic compounds such as Hydrogen Atom Transfer (HAT), Sequential Proton-Loss Electron Transfer (SPLET) and Single Electron Transfer (SET) [20], we tested compounds in the DPPH scavenging test, a commonly used antioxidant assay [21]. This method determines the capacity of compounds for neutralize radicals, regardless its biological importance; however, it is a preliminary test to identify novel and potential antioxidant entities. As shown in Table 1, none of the analogues lacking a hydroxyl group in the hydrazone ring had an observable response (compounds **3d**–**3f**), while compound **3a**, whose only substituent is hydroxyl at *para* position, neither demonstrated a scavenging activity. The preceding observation clearly indicates that this group is a necessary but not a sufficient requirement for exhibiting and antioxidant effect. Surprisingly, however, the cinnamaldehyde derivative **3h** had a significant 90 % of DPPH scavenging, though it lacks of substituents at phenyl ring. The latter finding could be explained by the participation of additional hydrogen abstractions in other positions, such as the amidic hydrogen, which conducts to a stabilized radical intermediate [18]. On the other hand, compounds bearing two hydroxyl groups (**3b** and **3c**) or those derived from well-known antioxidant motifs (syringaldehyde, **3g**; coniferylaldehyde, **3i** and sinapinaldehyde, **3j**), also scavenged DPPH radical, ranging from 22 to 94 % of inhibition. Notably, analogues owning oxygen substituents at both 2 or 3 and 4 positions (**3b**, **3g** and **3i**–**3j**) were the most active and their IC_{50} are shown in Table 1. It is noteworthy that those derivatives had a similar or higher activity than ferulic and sinapinic acid as well as the potent flavonoid quercetin, while the antioxidant effect of **3b** and **3g** was on the same magnitude as vitamin E (Table 1).

Figure 3 shows some plausible mechanisms in which compounds would scavenge DPPH radical; after hydrogen abstraction caused by DPPH by a HAT pathway, the phenoxy radical can be stabilized through resonance within the phenyl ring and even with the hydrazone moiety. On the other hand, the hydrazone could donate an electron to DPPH radical (SET pathway) generating a cationic-radical species, which would eventually lose a proton to produce the identical radical intermediary as the HAT path.

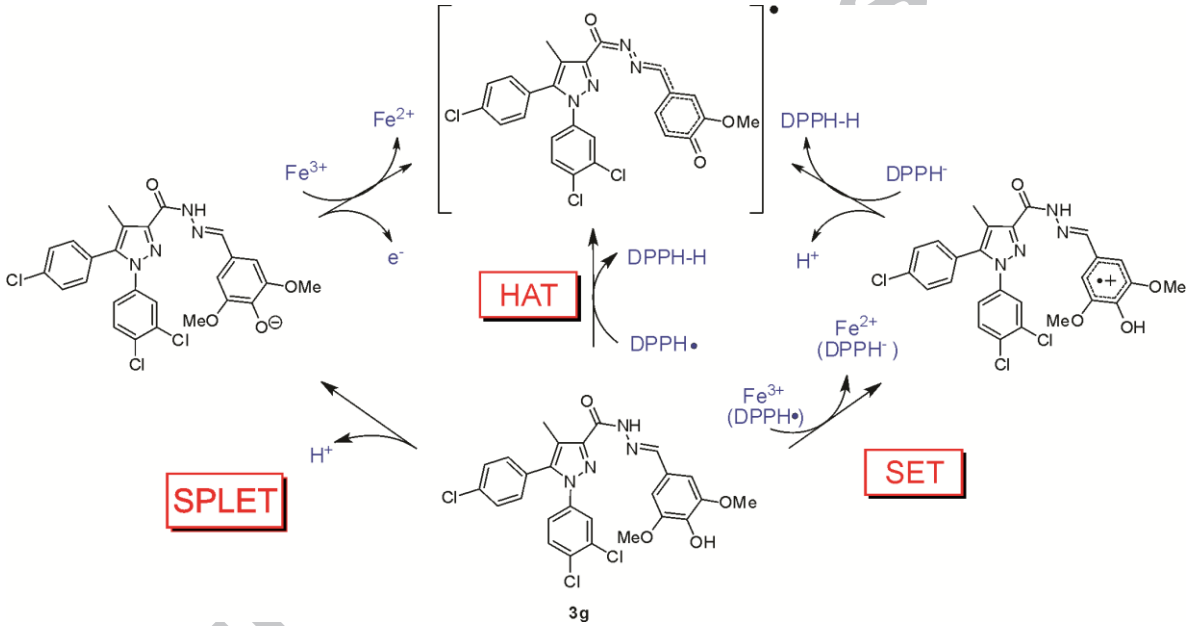

Figure 3. Schematization of several antioxidant mechanisms that might be attributed to *N´*-acylhydrazones **3a–3j**. The figure shows the most active compound **3g**.

Although some of the compounds (i.e. those derived from reported antioxidant portions) seemed to be excellent scavengers in DPPH test, such radical has no biological relevance. For this reason, we also evaluated the capacity of pyrazole derivatives **3a–3j** for reducing Fe^{3+} to Fe^{2+} by employing the ferric reducing antioxidant power (FRAP) test [22]. FRAP evaluates the antioxidant capacity by means of a SET or SPLET paths (Figure 3). Despite iron is essential for cellular metabolism, its accumulation may be a source of reactive species and thus oxidative stress [23, 24]. Similar findings were detected as in the case of the DPPH scavenging test: compounds lacking a hydroxyl

group at *para* position (**3d**–**3h**) had a minimum effect in reducing ferric to ferrous iron, expressed as trolox equivalents (μmmol Trolox/g of compound) (Figure 4). The same outcome was observed in the case of the 4-hydroxy derivative (**3a**) and the dihydroxylated (**3c**). However, the 4-hydroxy-3-methoxy derivatives **3g**, **3i** and **3j**, as well as the dihydroxylated **3b**, had the higher effect in reducing ferric iron, ranging from 20,046 to 45,667 trolox equivalents. Once more, the syringaldehyde derivative **3g** was the most active compound, reaching more than 45,000 trolox equivalents in FRAP test. It is important to highlight that we do not discard the possibility of compound **3b** to coordinate with iron, a well-documented antioxidant mechanism of catechol derivatives and polyphenols [25, 26].

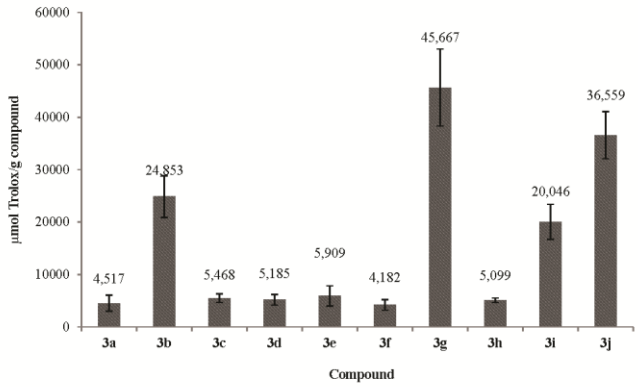

Figure 4. Antioxidant capacity of hydrazones **3a**–**3j** in FRAP test. Results are expressed as trolox equivalents (μmol trolox/g compound) ± SEM (n = 4)

2.2.2. Antidiabetic study

It is well-known that 3-carbonyl-1,5-diarylpyrazole compounds are selective CB1R antagonists, whose interaction with that receptor triggers several physiological responses, including glycemia reduction [27]. Moreover, the predicted pK_i (see Table 1) suggests that derivatives **3a**–**3j** are potential CB1R blockers. In order to confirm this hypothesis, we tested the compounds for their *in vivo* hypoglycemic capacity on an experimental noninsulin-dependent diabetes mellitus (NIDDM) model [28]. Compounds were evaluated at a dose of 50 mg/kg, which has been proven by our group to be suitable for discriminating among active and non-active candidates [29]. Figure 5 shows the plasma glucose reduction at 1, 3, 5 and 7 h after administration (for better understanding, the

derivatives were separated in two groups). It is note to worth that almost all pyrazole-3-carbohydrazides showed a biological response since 3 h after administration and was sustained until 7 h of the study, though the dimethoxy compound **3e** did not reduce the plasma glucose in any time of the antidiabetic experiment. This outcome clearly demonstrated that analogues must have a free hydroxyl group at 3 or 4 positions to exert a biological response. According to the later, compounds bearing a 4-hydroxy group (**3a**, **3b** and **3g**) showed a glucose reduction higher than 50 % at 7 hours after administration activity (70, 67 and 83 % of reduction for **3a**, **3b** and **3g**, respectively) and were even more active that the lead **2**. Gratifyingly, there exists a correlation between the antioxidant capacity and the glycemia reduction, in which the best antioxidant derivatives **3b** and **3g** also demonstrated the higher glucose reduction. The increasing in the biological effect could be attributed to either the enhancement of the affinity to CB1R or to the antioxidant capacity, which could reduce oxidative stress that is involved in the development and progression of diabetes. Surprisingly, however, the benzodioxane derivative **3f** was also active in the *in vivo* model, though it lacks of hydroxyl groups in its structure. One hypothesis for this unexpected phenomenon is that **3f** could suffer and oxidative dealkylation to produce a hydroxylated compound and thus enhance the affinity to CB1R; however, further experimentation must be done to corroborate it. On the other hand, the cinnamaldehyde derivatives showed a lower glycemia reduction than the lead **2** and therefore demonstrating that the vinylogation of the hydrazone moiety in this kind of compounds negatively impacts the biological effect, probably due to disfavored interactions with CB1R. In summary, compounds **3a**, **3b**, **3f** and **3g** are promising candidates for further optimization in the search for more potent antidiabetic compounds, especially those with an intrinsic antioxidant capacity (i.e. **3b** and **3g**) because of their potential to lessen the complications of metabolic syndrome and diabetes associated with oxidative stress.

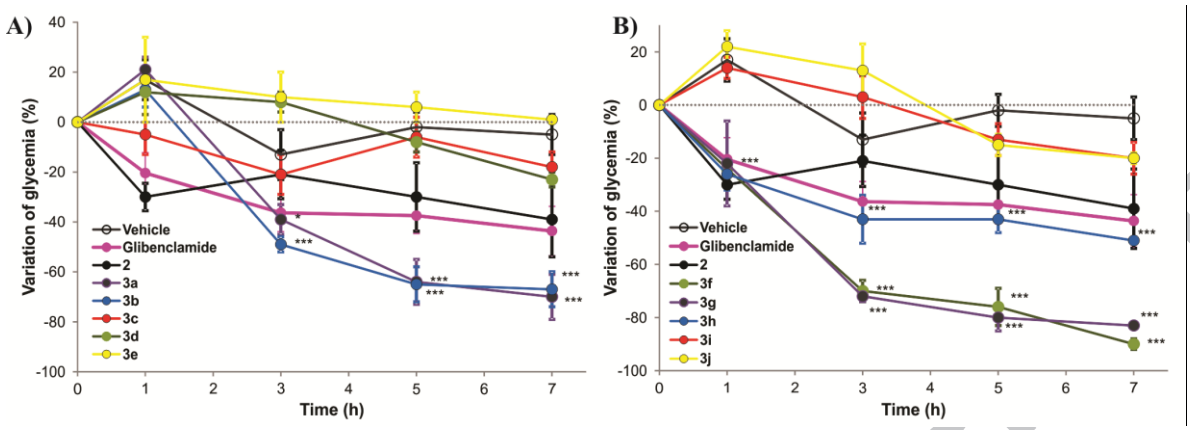

Figure 5. Effect of a single dose of hydrazones **3a–3e** (A) and **3f–3j** (B) in a streptozotocin/nicotinamide rat model of diabetes (50 mg/kg; intragastric, n = 5). *p < 0.05; **p < 0.01; ***p < 0.001.

2.3. Molecular docking study

In order to corroborate the possible mechanism of action of pyrazole derivatives and understand the detailed ligand-receptor interactions, we carried out a molecular docking study in a previously published CB1R [17]. Such G protein-coupled receptor (GPCR) was modeled by using the B chain of β1-adrenergic receptor from *Meleagris gallopavo* (PDB: 4AMJ, resolution of 2.30) [30] in the SWISSMODEL workspace [31]. Compounds were docked into the binding site of CB1 model using Autodock 4.2 program. The binding pose of each compound was selected according the existence of a hydrogen bond between the carbonyl moiety of hydrazones with Lys192, which is reported to be a crucial interaction for inverse agonist response [32]. Accordingly, the binding modes of the top-score docking poses are shown in Figure 5. With exception of compound **3j**, all analogues were satisfactorily docked into the binding site of CB1R with exothermic ΔG values (Table 2). Satisfyingly, compounds show a similar pose as rimonabant does [33], in which the carbonyl group interacts with Lys192 through a hydrogen bond and the aromatic rings point to a hydrophobic domain comprising Phe170, 174, 177 and 200, TRP356 and Ile277 (Figure 6). It is note to worth that a π-π stacking interaction is detected between Phe170 and the aromatic rings at 1 and 5 positions of the pyrazole ring. These similarities suggest that the derivatives described in this work could reduce the plasma

glucose by CB1R interaction in the peripheral tissues [34]. Nonetheless, there is no relationship between the binding energies and the observed hypoglycemic effect (Table 2) as the inactive compound **3e** also had a negative ΔG value (-10.2 kcal/mol) which was even higher than those calculated for the most active compounds **3b** and **3g** (-9.62 and -9.79 kcal/mol, respectively). Notwithstanding, several asseverations can be concluded from Figure 6; first the cinnamaldehyde derivatives **3h** and **3i** had a different conformation in the binding pocket of CB1R while **3j** could not be docked satisfactorily. This finding can be a plausible explanation of the moderate hypoglycemic activity of those analogues. Similarly, the bicyclic analogue **3f** also showed the same pose and thus a moderate activity is expected; contrarily, **3f** was one of the most potent compounds so that the hypothesis of the enhancement of activity through metabolic dealkylation is supported. On the other hand, the most active analogues had an additional interaction with Asn187, which is more significant in hydroxy than alkoxy substituents. The last observation could explain the increased hypoglycemic effect of **3b** and **3g** when compared with the 4-methoxy derivatives **3d** and **3e**. Although we proposed a plausible explanation to the observed biological effect in base of the computational outcomes, experimental CB1R binding assay is required to confirm the mechanism of action of derivatives **3a**–**3j**; those studies are currently underway in our laboratory.

Table 2. ΔG_{bind} of hydrazones **3a**–**3j** and rimonabant.

Compound	ΔG_{bind} (kcal/mol)
3a	-9.99
3b	-9.62
3c	-9.42
3d	-9.38
3e	-10.2
3f	-9.87
3g	-9.79
3h	-10.35
3i	-9.51
3j	--
Rimonabant (2)	-9.81

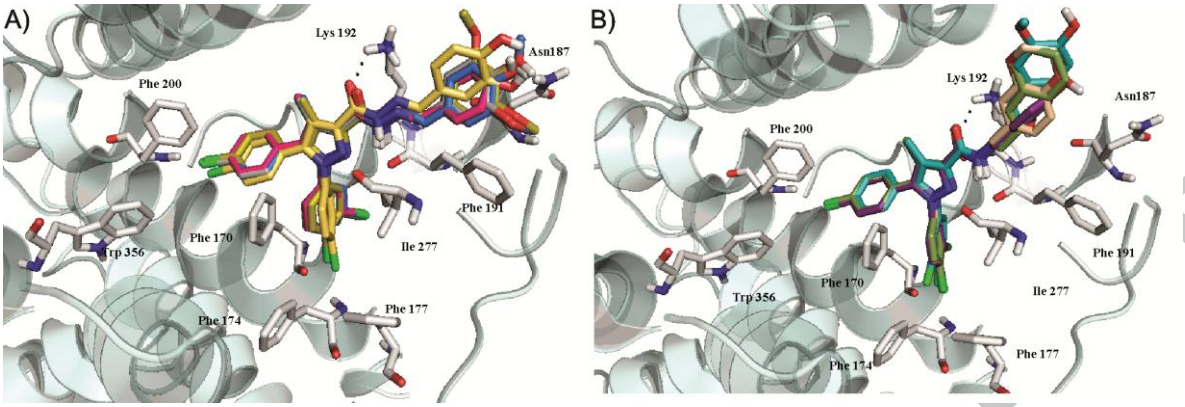

Figure 6. Predicted poses of hydrazones **3a**–**3j** inside the binding pocket of CB1R. Dashed lines illustrate hydrogen bonds between the carbonyl group and Lys192

Finally, the two-dimensional complex diagrams for rimonabant (**1**) and the most active **3g** obtained from the Poseview server [35] are shown in Figure 7. Both pyrazole derivatives share the hydrogen bond with Lys192 and the hydrophobic interactions with Phe170 (π-π stacking). However, it was soon discovered that compound **3g**, as described previously, possesses another hydrogen bond with Asn187, interaction that would enhance the affinity to CB1R and thus increasing the hypoglycemic effect. Summarizing, we demonstrated that compounds would act as dual entities by scavenging radicals through HAT and SET mechanisms and also reducing the glycemia in diabetic rats *via* blockade of CB1R and become excellent candidates for further optimization and investigation.

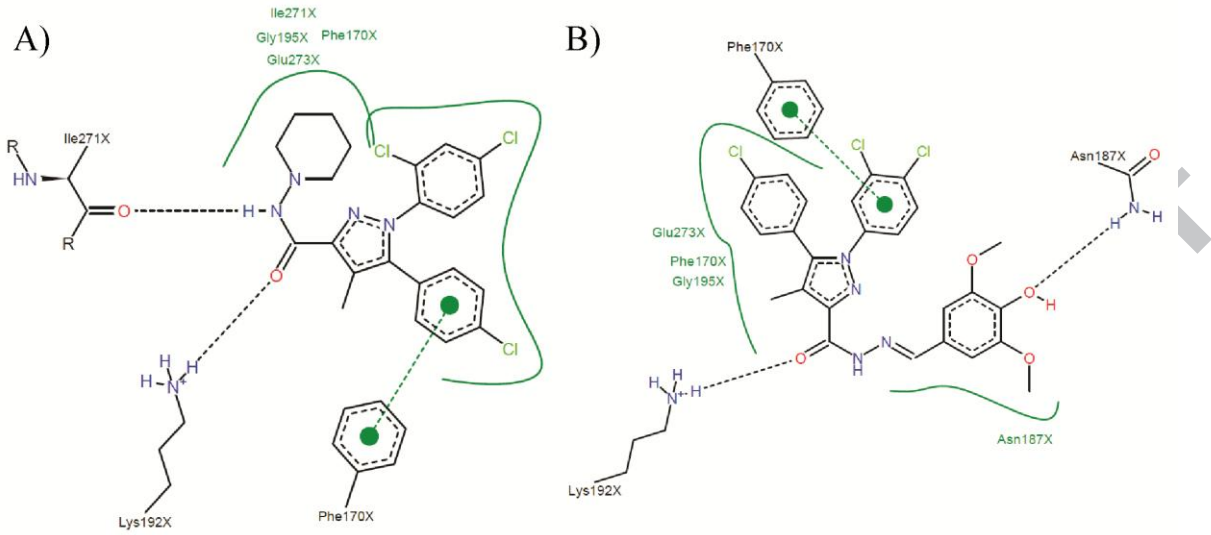

Figure 7. Two-dimensional complex diagrams of the binding pose of **1** (A) and compound **3g** (B) inside the binding pocket of CB1R.

3. Conclusions

Considering the close relationship between diabetes mellitus and metabolic syndrome, as well as their association with oxidative stress, ten hybrids of CB1R antagonists were designed and synthesized. The analogues included different hydroxylated patterns as a key feature for antioxidant capacity. Accordingly, hydrazones from well-known antioxidant portions among with the 3,4-dihydroxylated **3b** were demonstrated to be potent antioxidant compounds by scavenging DPPH radical and reducing Fe^{3+} to Fe^{2+} through HAT and SET mechanisms. Surprisingly, the IC_{50} of **3g** has the same order of magnitude than the effective α-tocopherol and was more potent than quercetin. Regarding the experimental NIDDM model, cinnamaldehyde-containing analogues showed lower activity than the lead **2** and the dimethoxylated **3e** lacked of biological effect. Contrarily, compounds with a 4-hydroxy moiety on the hydrazone ring exhibited a remarkable glycemia reduction and was more prominent than rimonabant and the lead **2**. The most active compounds were the potent antioxidants **3b** and **3g** (70 and 83 % of glycemia reduction, respectively), the phenolic **3a** (70 %) and, surprisingly, the benzodioxane derivative **3f**, with a 90 % of plasma glucose reduction, probably due to a metabolic dealkylation. Molecular docking on a previously modeled CB1R showed that compounds would interact with this GPCR in a similar way as rimonabant does, revealing a hydrogen bond with Lys192 and the aromatic rings interacting with

a phenylalanine-rich domain. Additionally, cinnamaldehyde derivatives possess a different conformation that could account for the reduction in biological response, while the hydroxylated analogues could interact with Asn187 through a hydrogen bond, a new proposed feature to enhance the affinity to CB1R and increase the hypoglycemic effect. The results presented in this work clearly corroborate the importance of considering CB1R as a biological target for the generation of more potent hypoglycemic compounds for the treatment of diabetes and metabolic syndrome, and place hydrazones **3a**–**3j** as interesting antioxidant and antidiabetic entities.

4. Experimental

4.1. Chemistry

Solvents and reagents were purchased from Sigma-Aldrich and were used without purification. Melting points were determined on a Büchi melting point apparatus, model B-540 and are uncorrected. The progress of reactions and the purity of final products were monitored by thin layer chromatography (TLC) whereas UV and iodine oxidation were used as revealing agents. ^{1}H and ^{13}C NMR spectra were obtained in DMSO-*d6* and $CDCl_3$ solutions at 400 MHz (for ^{1}H) and 100 MHz (for ^{13}C) on a Varian MR-400 (9.2 T) instrument and on a Varian VNMRS-400 (9.2 T) instrument. Chemical shifts (δ) are reported in ppm relative to the solvent signal. Elemental analyses were conducted on a PerkinElmer® 2400 Series II CHNS/O instrument. Mass spectrometry spectra were obtained using a Thermo- electron model DFS instrument. Glibenclamide, nicotinamide, streptozotocin and Tween 80 were purchased from Sigma-Aldrich Co. (St. Louis, MO, USA).

4.1.1. Synthesis of lithium salt of ethyl 3-methyl-2,4-dioxo-4-(4-chlorophenyl)butanoate (**5**)

To a solution of 4-chloropropiophenone **4** (15.06 mmol) in 3 mL of anhydrous methylcyclohexane was added, at room temperature, a solution of lithium *bis*(trimethylsilyl)amide (16.1 mmol) in anhydrous methylcyclohexane (5 mL). After 3 h of stirring, diethyl oxalate (16.6 mmol) was added dropwise and then left to react for 16 h. The mixture was filtered and washed with several portions of methylcyclohexane and used in the next reaction without purification.

4.1.2. Synthesis of 5-(4-Chlorophenyl)-1-(3,4-dichlorophenyl)-4-methyl-1H-pyrazole-3-carboxylic acid (**6**)

A mixture of the lithium salt **5** (13.8 mmol) and substituted phenylhydrazine (15.6 mmol) was suspended in 50 mL of EtOH and H_2SO_4 was added dropwise in an ice bath. The mixture was heated to reflux and stirred until the starting material was completely consumed. The resulting solution was cooled to room temperature and the excess of ethanol was removed *in vacuo*. 20 mL of water were added and the suspension was neutralized with $NaHCO_3$ and then extracted with $CHCl_3$ (3 x 20 mL). The organic layer was successively dried over Na_2SO_4, filtered and concentrated *in vacuo.* The residue containing the ester product was then dissolved in 20 mL of EtOH and KOH (23 mmol) was added. The mixture was allowed to react 12 h at 50 °C. The resulting suspension was concentrated *in vacuo* and dissolved in 30 mL of water and later washed with hexane (3 x 15 mL). The aqueous layer was acidified with concentrated HCl until the pure carboxylic acids precipitated. Light brown solid in 82 % yield, mp 203–204 °C. **^{1}H NMR** (300 MHz, DMSO-d_6): δ 7.85 (d, *J* = 2.4 Hz, 1H, ArH), 7.67 (d, *J* = 8.7 Hz, 1H, ArH), 7.56 (d, *J* = 8.4 Hz, 2H, ArH), 7.36 (d, *J* = 8.4 Hz, 2H, ArH), 7.14 (dd, *J* = 8.8 and 2.4 Hz, 1H, ArH), 2.21 (s, 3H, CH_3). **MS (FAB)** m/z 381 [(M+1)+], 383 [(M+3)+], 385 [(M+5)+], 363[(M+1)-18].

4.1.3. General synthesis of N´-arylidene-5-(4-chlorophenyl)-1-(3,4-dichlorophenyl)-4-methyl-1H-pyrazole-3-carbohydrazides (**3a–3j**)

To a stirred solution of the 1,5-diarylpyrazole-3-carboxylic acid **6** (0.5 mmol) in 15 mL of toluene, $SOCl_2$ (0.2 mL) was slowly added. The mixture was heated to reflux for ca. 2.5. h. Then, the excess of solvent and $SOCl_2$ were removed *in vacuo* and the residue was dissolved in 10 mL of $CHCl_3$. To this stirred mixture at 0°C, a solution of *t*-butylcarbazate (0.55 mmol) and diisopropylethylamine (DIPEA, 0.55 mmol) in 10 mL of $CHCl_3$ was added dropwise. After the consumption of the acyl chloride, the chloroformic solution was subsequently washed with citric acid 0.5 M and saturated aqueous $NaHCO_3$. The combined organic extracts were filtered, dried over Na_2SO_4 and evaporated, which afforded the desired *N*-Boc carbohydrazide **7** in an acceptable purity.

The unpurified *N*-Boc carbohydrazide **7** was stirred with TFA (1 mL) at room temperature for 2.5 h. Once the deprotection was completed, the remnant TFA was co-distilled with 20 mL of $CHCl_3$ (this procedure was repeated two more times). Finally, to the resulting oil, $CHCl_3$ (20 mL) were added and the corresponding aldehyde (0.55 mmol) and catalytic acetic acid were aggregated. The solution was stirred for ca. 4 h at room temperature and then evaporated. The resulting mixture was purified by column chromatography on silica gel ($CHCl_3$ to $CHCl_3$–MeOH 9:1) to afford the desired carbohydrazydes **3a–3j**.

4.1.3.1. (*E*)-5-(4-chlorophenyl)-1-(3,4-dichlorophenyl)-*N′*-(4-hydroxybenzylidene)-4-methyl-1*H*-pyrazole-3-carbohydrazide (**3a**). Off-White solid in 82 % yield; mp 285–286 °C. **IR** (cm^{-1}): 3323, 3184, 3095, 2925, 1667, 1541, 1598, 1512, 1475, 1219.55; **^{1}H-NMR** ($DMSO_{-d6}$, δ ppm, 400 MHz): 2.23 (s, 3H, CH_3Ar), 6.85 (AA´BB´, 2H, ArH), 7.13 (dd, *J* = 8.8 and 2.4 Hz, 1H, ArH), 7.33 (AA´BB¨, 2H, ArH), 7.53–7.56 (comp, 4H, ArH), 7.65 (d, *J* = 8.8 Hz, 1H, ArH), 7.81 (d, *J* = 2.4 Hz, 1H, ArH), 8.43 (s, 1H, N=CH), 9.94 (s, 1H. ArOH), 11.56 (s, 1H, NH); **^{13}C-NMR** ($DMSO_{-d6}$, δ ppm, 100 MHz): 9.0, 115.8, 118.7, 124.9, 125.4, 127.0, 127.4, 128.8, 129.0, 130.6, 130.8, 131.6, 131.9, 134.0, 138.6, 140.9, 144.0, 148.2, 158.1, 159.4; **MS (EI)** m/z: 498; **Anal. calcd** for $C_{24}H_{17}Cl_3N_4O_2$ C,57.68; H, 3.43; N, 11.21; found C, 58.17; H, 2.81; N, 11.43.

4.1.3.2. (*E*)-5-(4-chlorophenyl)-1-(3,4-dichlorophenyl)-*N′*-(3,4-dihydroxybenzylidene)-4-methyl-1*H*-pyrazole-3-carbohydrazide (**3d**). White solid in 83 % yield; mp 244–245 °C. **IR** (cm^{-1}): 3561, 3542, 3131, 1666, 1514.93, 1590, 1475, 1288.01; **^{1}H-NMR** ($DMSO_{-d6}$, δ ppm, 400 MHz): 2.23 (s, 3H, CH_3Ar), 6.79 (d, *J* = 8 Hz, 1H, ArH), 6.92 (dd, *J* = 8.4 and 2 Hz, 1H, ArH), 7.13 (dd, *J* = 8.6 and 2.4 Hz, 1H, ArH), 7.23 (d, *J* = 2 Hz, 1H, ArH), 7.34 (AA´BB´, 2H, ArH), 7.54 (AA´BB´, 2H, ArH), 7.66 (d, *J* = 8.8 Hz, 1H, ArH), 7.81 (d, *J* = 2.4 Hz, 1H, ArH), 8.35 (s, 1H, N=CH), 9.30 (br s, 1H, ArOH), 9.34 (br s, 1H, ArOH); 11.51 (s, 1H, NH); **^{13}C-NMR** ($DMSO_{-d6}$, δ ppm, 100 MHz): 9.0, 112.7, 115.6, 118.6, 120.5, 124.9, 125.8, 126.9, 127.4, 129.0, 130.6, 130.8, 131.6, 131.9, 134.0, 138.6, 140.8, 144.0, 145.7, 147.9, 148.4, 158.1; **MS (EI)** m/z: 514; **Anal. calcd** for $C_{24}H_{17}Cl_3N_4O_3$ C,55.89; H, 3.32; N, 10.86; found C, 55.86; H, 2.76; N, 11.08.

4.1.3.3. (*E*)-5-(4-chlorophenyl)-1-(3,4-dichlorophenyl)-*N′*-(2,4-dihydroxybenzylidene)-4-methyl-1*H*-pyrazole-3-carbohydrazide (**3c**) Beige solid in 75 % yield; mp 275–275 °C. **IR** (cm^{-1}): 3321, 3252, 3093, 2978, 1669, 1536, 1536, 1477, 1217; **^{1}H-NMR** ($DMSO_{-d6}$, δ ppm, 400 MHz): 2.24 (s, 3H,

CH_3Ar), 6.32 (d, *J* = 2.4 Hz, 1H, ArH), 6.37 (dd, *J* = 8.4 and 2.4 Hz, 1H, ArH), 7.14 (dd, *J* = 8.6 and 2.4 Hz, 1H, ArH), 7.25 (d, *J* = 8.4 Hz, 1H, ArH), 7.34 (AA´BB´, 2H, ArH), 7.54 (AA´BB´, 2H, ArH), 7.67 (d, *J* = 8.8 Hz, 1H, ArH), 7.82 (d, *J* = 2.4 Hz, 1H, ArH), 8.61 (s, 1H, N=CH), 9.96 (s, 1H, ArOH), 11.52 (s, 1H, ArOH), 11.90 (s, 1H, NH); **^{13}C-NMR** ($DMSO_{-d6}$, δ ppm, 100 MHz): 8.9, 102.7, 107.7, 110.5, 118.7, 124.8, 127.0, 127.3, 129.0, 130.6, 130.8, 131.4, 131.5, 131.8, 138.6, 139.0, 140.9, 143.5, 149.5, 157.8, 159.5, 160.6; **MS (EI)** m/z: 514; **Anal. calcd** for $C_{24}H_{17}Cl_3N_4O_3$ C,55.89; H, 3.32; N, 10.86; found C, 56.07; H, 2.51; N, 11.32.

4.1.3.4. (*E*)-5-(4-chlorophenyl)-1-(3,4-dichlorophenyl)-N'-(3-hydroxy-4-methoxybenzylidene)-4-methyl-1*H*-pyrazole-3-carbohydrazide (**3d**). White solid in 78 % yield; m.p. 240242 °C**. IR** (cm^{-1}) 3530, 3172, 3074, 1646, 1602, 1511, 1377, 1279, 1095; **^{1}H-NMR** ($DMSO_{-d6}$, δ ppm, 400 MHz): 2.24 (s, 3H, CH_3Ar), 3.81 (s, 3H, OCH_3), 6.98 (d, *J* = 8.4 Hz, 1H, ArH), 7.04 (dd, *J* = 8.4 and 2 Hz, 1H, ArH), 7.13 (dd, *J* = 2.4 and 8.6 Hz, 1H, ArH), 7.26 (d, *J* = 2 Hz, 1H, ArH), 7.34 (AA´BB´, 2H, ArH), 7.55 (AA´BB´2H, ArH), 7.67 (d, *J* = 8.8 Hz, 1H, ArH), 7.82 (d, *J* = 2.8 Hz, 1H, ArH), 8.37 (s, 1H, N=CH), 9.33 (s,1H, ArOH), 11.59 (s, 1H, NH); **^{13}C-NMR** ($DMSO_{-d6}$, δ ppm, 100 MHz): 9.0, 55.6, 111.9, 112.3, 118.6, 120.2, 124.9, 127.0, 127.2, 127.4, 129.0, 130.6, 130.8, 131.6, 131.9, 134.0, 138.6, 140.9, 143.9, 146.9, 148.0, 149.8 158.2; **MS (EI)** m/z: 528; **Anal. calcd** for $C_{24}H_{19}Cl_3N_4O_3$ C,56.68; H, 3.61; N, 10.58; found C, 56.37; H, 3.31; N, 10.32.

4.1.3.5. (*E*)-5-(4-chlorophenyl)-1-(3,4-dichlorophenyl)-*N'*-(3,4-dimethoxybenzylidene)-4-methyl-1*H*-pyrazole-3-carbohydrazide (**3e**). Beige solid in 73 % yield; mp 233–234 °C. **IR** (cm^{-1}): 3184, 3078, 3007, 2959, 2933, 2839, 1648, 1512, 1575, 1479, 1265, 1240; **^{1}H-NMR** ($DMSO_{-d6}$, δ ppm, 400 MHz): 2.23 (s, 3H, CH_3Ar), 3.81 (s, 3H, CH_3O), 3.83 (s, 3H, CH_3O), 7.03 (d, *J* = 8.4 Hz, 1H, ArH), 7.14 (dd, *J*= 8.6 and 2.4 Hz, 1H, ArH), 7.17 (dd, *J* = 8.2 and 2 Hz, 1H, ArH), 7.34 (AA´BB´, 2H, ArH), 7.35 (m, 1H, ArH), 7.54 (AA´BB´, 2H, ArH), 7.66 (d, *J* = 8.8 Hz, 1H, ArH), 7.82 (d, *J* = 2.4 Hz, 1H, ArH), 8.46 (s, 1H, N=CH), 11.65 (s, 1H, NH); **^{13}C-NMR** ($DMSO_{-d6}$, δ ppm, 100 MHz): 9.0, 55.5, 55.6, 108.0, 111.5, 118.9, 122.0, 124.9, 127.0, 127.1, 127.4, 129.0, 130.6, 130.8, 131.6, 131.9, 134.0, 138.6, 140.9, 143.9, 148.0, 149.1, 150.8, 158.2. **MS (EI)** m/z: 542; **Anal. calcd** for $C_{26}H_{21}Cl_3N_4O_3$ C,57.42; H, 3.89; N, 10.30; found C, 57.56; H, 3.89; N, 10.50.

4.1.3.6. (*E*)-5-(4-chlorophenyl)-1-(3,4-dichlorophenyl)-*N'*-((2,3-dihydrobenzo[*b*][1,4]dioxin-6-yl)methylene)-4-methyl-1*H*-pyrazole-3-carbohydrazide (**3f**). Off-white solid in 68 % yield; mp 205–

206 °C. **IR** (cm^{-1}): 3330, 1549, 3064), 2923, 2876, 1670, 1506, 1477, 1259, 1240; **^{1}H-NMR** ($DMSO_{-d6}$, δ ppm, 400 MHz): 2.23 (s, 3H, CH_3Ar), 4.28 (br s, 4H, $(CH_2O)_2$), 6.94 (d, *J* = 8.4 Hz, 1H, ArH), 7.14 (dd, *J* = 8.8 and 2.8 Hz, 1H, ArH), 7.17–7.21 (comp, 2H, ArH), 7.34 (AA´BB´, 2H, ArH), 7.55 (AA´BB´, 2H, ArH), 7.66 (d, *J* = 8.8 Hz, 1H, ArH), 7.82 (d, *J* = 2.8 Hz, 1H, ArH), 8.42 (s, 1H, N=CH), 11.65 (s, 1H, NH); **^{13}C-NMR** ($DMSO_{-d6}$, δ ppm, 100 MHz): 9.0, 64.0, 64.3, 115.2, 117.5, 118.7, 120.7, 124.8, 126.9, 127.4, 127.8, 129.0, 130.6, 130.8, 131.6, 131.9, 134.0, 138.6, 140.9, 143.6, 143.9, 145.2, 147.5, 158.2; **MS (EI)** m/z: 540; **Anal. calcd** for $C_{26}H_{19}Cl_3N_4O_3$ C,57.64; H, 3.53; N, 10.34; found C, 57.89; H, 2.82; N, 10.46.

4.1.3.7. (*E*)-5-(4-chlorophenyl)-1-(3,4-dichlorophenyl)-*N*′-(4-hydroxy-3,5-dimethoxybenzylidene)-4-methyl-1*H*-pyrazole-3-carbohydrazide (**3g**). Yellowish solid in 54 % yield; mp 269–279 °C. **IR** (cm^{-1}): 3252, 3087, 3059, 2955, 2933, 2836, 1667, 1554, 1512, 1477, 1209; **^{1}H-NMR** ($DMSO_{-d6}$, δ ppm, 400 MHz): 2.23 (s, 3H, CH_3Ar), 3.83 (s, 6H, OCH_3), 6.97 (s, 2H, ArH), 7.13 (dd, *J* = 8.6 and 2.4 Hz, ArH), 7.34 (AA´BB´, 2H, ArH), 7.65 (AA´BB´, 2H, ArH), 7.66 (d, *J* = 8.8 Hz, 1H, ArH), 7.82 (d, *J* = 2.4 Hz, 1H, ArH), 8.41 (s, 1H, N=CH), 8.91 (s, 1H, ArOH), 11.63 (s, 1H, NH); **^{13}C-NMR** ($DMSO_{-d6}$, δ ppm, 100 MHz): 9.0, 56.0, 104.5, 118.6, 124.6, 124.9, 127.0, 127.4, 129.1, 130.6, 130.8, 131.6, 131.9, 134.0, 137.9, 138.6, 140.9, 144.0, 148.1, 148.5, 158.2; **MS (EI)** m/z: 558; **Anal. calcd** for $C_{26}H_{21}Cl_3N_4O_4$ C,55.78; H, 3.78; N, 10.01; found C, 56.13; H, 3.19; N, 10.21.

4.1.3.8. (*E*)-5-(4-chlorophenyl)-1-(3,4-dichlorophenyl)-4-methyl-*N*′-((*E*)-3-phenylallylidene)-1*H*-pyrazole-3-carbohydrazide (**3h**). White solid in 58 % yield; mp 163–164 °C. **IR** (cm^{-1}): 3381, 3001, 3027, 3060, 2925, 1655, 1548, 1477; **^{1}H-NMR** ($DMSO_{-d6}$, δ ppm, 400 MHz): 2.23 (s, 3H, CH_3Ar), 7.00 (d, *J* = 16 Hz, 1H, ArCH=CH), 7.07 (dd, *J* = 16 and 8.4 Hz, 1H, ArCH=CH), 7.14 (dd, *J* = 8.6 and 2.4 Hz, 1H, ArH), 7.35–7.31 (comp, 3H, ArH), 7.42–7.38 (m, 2H, ArH), 7.54 (AA´BB´, 2H, ArH), 7.64–7.62 (m, 2H, ArH), 7.67 (d, *J* = 8.8 Hz, 1H, ArH), 7.81 (d, *J* = 2.4 Hz, 1H, ArH), 8.33 (d, *J* = 8 Hz, 1H, N=CH), 11.69 (s, 1H, NH); **^{13}C-NMR** ($DMSO_{-d6}$, δ ppm, 100 MHz): 9.0, 118.7, 125.0, 125.8, 127.08, 127.1, 127.4, 128.8, 129.0, 130.7, 130.8, 131.6, 131.9, 134.0, 135.9, 138.6, 138.9, 140.9, 143.8, 149.8, 158.3; **MS (EI)** m/z: 508; **Anal. calcd** for $C_{26}H_{19}Cl_3N_4O$ C,61.25; H, 3.76; N, 10.99; found C, 61.74; H, 3.22; N, 10.10.

4.1.3.9. (*E*)-5-(4-chlorophenyl)-1-(3,4-dichlorophenyl)-*N*′-((*E*)-3-(4-hydroxy-3-methoxyphenyl)allylidene)-4-methyl-1*H*-pyrazole-3-carbohydrazide (**3i**). Orange solid in 47 % yield;

mp 213–214 °C. **IR** (cm^{-1}): 3536, 3252, 3093, 2966, 2940, 2842, 1668, 1528, 1593, 1475, 1208; **^{1}H-NMR** ($DMSO_{-d6}$, δ ppm, 400 MHz): 2.23 (s, 3H, CH_3Ar); 3.82 (s, 3H, OCH_3), 6.78 (d, *J* = 8 Hz, 1H, ArH), 6.87 (d, *J* = 16.4 Hz, 1H, ArCH=CH), 6.96 (dd, *J* = 16 and 8 Hz, 1H, ArCH=CH); 7.03 (dd, *J* = 8.2 and 2 Hz, 1H, ArH), 7.15 (dd, *J* = 8.8 and 2.4Hz, 1H, ArH), 7.2 (d, *J* = 2 Hz, 1H, ArH), 7.33 (AA´BB, 2H, ArH), 7.54 (AA´BB´, 2H, ArH), 7.67 (d, *J* = 8.6 Hz, 1H, ArH), 7.81 (d, *J* = 2.4 Hz, 1H, ArH), 8.28 (d, *J* = 8.4 Hz, 1H, N=CH), 9.36 (s, 1H, ArOH), 11.58 (s, 1H, NH); **^{13}C-NMR** ($DMSO_{-d6}$, δ ppm, 100 MHz): 9.0, 55.6, 110.2, 115.6, 118.6, 121.3, 122.8, 124.9, 127.0, 127.4, 127.6, 129.0, 130.6, 130.8, 131.6, 131.9, 134.0, 138.6, 139.5, 140.9, 143.9, 147.8, 147.9, 150.4, 158.1; **MS (EI)** m/z: 554; **Anal. calcd** for $C_{27}H_{21}Cl_3N_4O_3$ C,58.34; H, 3.81; N, 10.08; found C, 58.43; H, 3.99; N, 9.66.

4.1.3.10. (*E*)-5-(4-chlorophenyl)-1-(3,4-dichlorophenyl)-*N*′-((*E*)-3-(4-hydroxy-3,5-dimethoxyphenyl)allylidene)-4-methyl-1*H*-pyrazole-3-carbohydrazide (**3j**). Yellow solid in 61 % yield; mp 249–250 °C; **IR** (cm^{-1}):3276, 3072, 3030, 2989, 2960, 2937, 2837, 1666, 1540, 1594, 1515, 1252, 1201; **^{1}H-NMR** ($DMSO_{-d6}$, δ ppm, 400 MHz): 2.23 (s, 3H, CH_3Ar), 3.81 (s, 6H, CH_3O), 6.88 (d, *J* = 16 Hz, 1H, ArCH=CH), 6.92 (s, 2H, ArH), 7.01 (dd, *J* = 25.8 and 9.2Hz, 1H, ArCH=CH), 7.14 (dd, *J* = 8.6 and 2.4 Hz, 1H, ArH), 7.33 (AA´BB, 2H, ArH), 7.54 (AA´BB´, 2H, ArH), 7.66 (d, *J* = 8.4 Hz, 1H, ArH), 7.81 (d, *J* = 2.4 Hz, 1H, ArH), 8.29 (d, *J* = 8.8 Hz, 1H, N=CH), 8.73 (s, 1H, ArOH), 11.59 (s, 1H, NH); **^{13}C-NMR** ($DMSO_{-d6}$, δ ppm, 100 MHz): 9.1, 56.0, 104.8, 118.7, 123.4, 125.0, 126.5, 127.1, 127.4, 129.0, 130.6, 130.8, 131.6, 131.9, 134.0, 136.8, 138.6, 139.7, 140.9, 143.9, 148.1, 150.3, 158.1; **MS (EI)** m/z: 584; **Anal. calcd** for $C_{28}H_{23}Cl_3N_4O_4$ C,57.40; H, 3.96; N, 9.56; found C, 57.91; H, 3.72; N, 9.28.

4.2. *In vitro* antioxidant assays

4.2.1. DPPH-scavenging test

DPPH radical scavenging activity was investigated according to the method of Sreejayan and Rao [36]. Briefly, 2.95 mL of ethanolic solution of 100 μM DPPH and 0.05 mL of samples at different concentrations were mixed. The control tube contains distilled water instead of sample. After

incubation for 20 min at room temperature and in darkness the absorbance at 517 nm was recorded. The antioxidant capacity is given as percent (%) DPPH scavenging, calculated as [(optical density of control – optical density of sample)/(optical density of control) x 100]. The samples where measured by triplicate and the results are represented as mean± standard error (SEM).

4.2.2. FRAP test

The FRAP assay was conducted in accordance with Benzie & Strain with some modifications [37]. Briefly FRAP reagent was prepared by mixing 2.5 mL of TPTZ in HCl (40 mM), 2.5 g of $FeCl_3.6H_2O$ (20 mM) and 25 mL of acetate buffer (300 mM, pH = 3.6). Afterwards, 30 μL of samples at different concentrations or Trolox standards/vehicle, 90 μL of deionizated water and 900 μL of FRAP solution mixture were mixed and left at rest in the dark for 30 min at 37 ºC. The absorbance of the samples was measured in comparison to a blank at a wavelength of 595 nm. The FRAP values were calculated using the net area under the curves and were expressed as μmoles of Trolox equivalents per gram of samples.

4.3. Animals

Male Wistar rats with 200–250 g of body weight were housed at standard laboratory conditions (22 ± 3 °C, 12 h day/night cycle), fed with a rodent pellet diet and water ad libitum. Animals described as 'fasted' were deprived of food for 16 h, but had free access to water. All animal procedures were conducted in accordance with Federal Regulations for Animal Experimentation and Care (NOM-062-ZOO-1999, SAGARPA, Mexico) and approved by the Institutional Animal Care and Use Committee based on the US National Institute for Health (publication No. 85-23, revised 1985).

4.4. Induction of diabetes

Diabetes was induced in overnight fasted rats by intraperitoneal (i.p.) injection of 110 mg/kg of nicotinamide 15 min before an i.p. injection of 65 mg/kg of streptozotocin dissolved in cold citrate buffer (pH 4.5). Rats with hyperglycemia (i.e. those with blood glucose between 200 and 350 mg/dL) were detected after 72 h using a glucometer and these were used for antidiabetic screening.

4.5. Antidiabetic model

All compounds (50 mg/kg) were dissolved in Tween 80 at 10% in water (vehicle) and administered intragastrically to groups of five diabetic rats; control groups of vehicle (1 mL/rat) and glibenclamide (5 mg/kg) were also administered for negative control and drug reference. Blood samples were collected from the tail vein at 0, 3, 5 and 7 h after administration and glucose was measured using a commercial glucometer. The percentage of glycemia variation was calculated in relation to initial levels (0 h) using the formula: % variation of glycemia = [(Gx-G0) / G0] X 100, where G0 were the initial glycemia values and Gx were the glycemia values at 1, 3, 5 and 7 h, respectively. All values are expressed as mean ± S.E.M. the significance was estimated by an analysis of variance (ANOVA), $p< 0.05$ implies significance [38].

Acknowledgments

Financial support from the Instituto de Ciencia y Tecnología del Distrito Federal (ICYTDF235/2010) is acknowledged. Eduardo Hernández-Vázquez is granted to the CONACyT for his fellowship (number 216082). We also thank to Rosa Isela del Villar, Georgina Duarte, Margarita Guzmán and Marisela Gutiérrez for the analytical support.

References

[1] Akbas, F.; Gasteyger, C.; Sjödin, A; Astrup, A.; Larsen, T. M. Obes. Rev. 2009, 10, 58.

[2] Mackie, K. Annu. Rev. Pharmacol. Toxicol. 2006, 46, 101.

[3] For recent works concerning CB1R antagonists, see: a) Fulp, A.; Zhang, Y.; Bortoff, K.; Seltzman, H.; Snyder, R.; Wiethe, R.; Amato, G.; Maitra, R. Bioorg. Med. Chem. 2016, 24, 1063. b) German, N.; Decker, A. M.; Gilmour, B.; Gay, E.; Wiley, J.; Thomas, B.; Zhang, Y. J. Med. Chem. 2014, 57, 7758. c) Alvarado, M.; Decara, J.; Luque, M.J.; Hernández-Folgado, L.; Gómez-Cañas, M.; Gómez-Ruiz, M.; Fernández-Ruiz, J.; Elguero, J.; Jagerovic, N.; Serrano, A.; Rodríguez de Fonseca, F.; Bioorg. Med. Chem. 2013, 21, 1708. d) Fulp, A.; Bortoff, K.; Seltzman, H.; Zhang, Y.; Mathews, J.; Snyder, R.; Fennell, T. J. Med. Chem. 2012, 55, 2820. e) Cluny, N. L.; Vemuri, V. K.; Chambers, A. P.; Limebeer, C. L.; Bedard, H.; Wood, J. T.; Lutz, B.; Zimmer, A.; Parker, L. A.; Makriyannis, A.; Sharkey, K. A. Br. J. Pharmacol. 2010, 3, 629.

[4] Crespo, I.; Gómez de Heras, R.; Rodríguez de Fonseca, F.; Navarro, M. Neuropharmacology 2008, 54, 219.

[5] Tam, J.; Verumi, V. K.; Liu, J.; Bátkau, S.; Mukhopadhyay, B.; Godlewsky, G.; Osei-Hyiaman, D.; Ohnuma, S.; Ambudkar, S. V.; Pickel, J.; Makriyannis, A.; Kunos, G. J. Clin. Invest. 2010, 120, 2953.

[6] Bellocchio, L.; Cervino, C.; Pasquali, R.; Pagotto, U. J. Neuroendocrinol. 2008, 20, 130–138.

[7] Hernández-Vázquez, E.; Méndez-Lucio, O.; Hernández-Luis, F. Med. Chem. Res. 2013, 22, 4133.

[8] Engeli, S. Obesity Facts 2008, 1, 8.

[9] Bifulco, M.; Pisanti, S. Nat Rev Drug Discov. 2009, 8, 594.

[10] Maritim, A. C.; Sanders, R. A.; Watkins, J. B. J. Biochem Mol. Toxicol. 2003, 7, 24.

[11] Ceriello, A. Metabolism 2000, 49, 27.

[12] Evans, J. L.; Goldfine, I. R.; Maddux, B. A.; Grodssky, G. M. Diabetes 2003, 53, 1.

[13] Bierhaus, A.; Schiekofer, S.; Schwaninger, M.; Andrassy, M.; Humpert, P. M.; Chen, J.; Hong, M.; Luther, T.; Henle, T.; Kloting, I.; Morcos, M.; Hofmann, M.; Tritschler, H.; Weigle, B.; Kasper, B.; Smith, M.; Perry, G.; Schmidt, A. M.; Stern, D. M.; Haring, H. U.; Schleicher, E.; Nawroth, P. P. Diabetes 2001, 50, 2792.

[14] Rains, J. L.; Jain, S. K. Free Radic. Biol. Med. 2011, 50, 567.

[15] Hayden, M. R.; Tyagi, S. C. JOP 2002, 3, 86.

[16] Wiernsperger, N. F. Diabetes Metab. 2003, 29, 579.

[17] Hernández-Vázquez, E.; Aguayo-Ortiz, R.; Ramírez-Espinosa, J. J.; Estrada-Soto, S.; Hernández-Luis, F. Eur. J. Med. Chem. 2013, 69, 10.

[18] Hernández-Vázquez, E.; Castañeda-Arriaga, R.; Ramírez-Espinosa, J. J.; Medina-Campos, O. M.; Hernández-Luis, F.; Pedraza-Chaverri, J.; Estrada-Soto, S. Eur. J. Med. Chem. 2015, 100, 106.

[19] Chen, J. Z.; Han, X. W.; Liu, Q.; Makriyannis, A.; Wang, J.; Xie, X. Q, J. Med. Chem. 2006, 49, 625.

[20] Litwinienko, G.; Ingold, K. U. Acc. Chem. Res. 2007, 40, 222.

[21] a) Miranda, L. D.; Hernández-Vázquez, E. J. Org. Chem. 2015, 80, 10611. b) Patil, A. B.; Ghosh, S.; Phadatare, S. D.; Pathak, P.; Sharma, G.; Chopade, B.; Shinde, V. S. New J. Chem. 2015, 39, 1267. c) Reddy, K. K.; Ravinder, T.; Prasad, R. B.; Kanjilal, S. J. Agric. Food Chem. 2011, 59, 564.

[22] a) Rehakova, Z.; Koleckar, V.; Jahodar, L.; Opletal, L.; Macakova, K.; Cahlikova, L.; Jun D, Kuca, K. J. Enzyme Inhib. Med. Chem. 2014, 1, 49. b) Kashima, Y.; Miyazawa, M. Arch. Pharm. Res. 2012, 35, 1533. c) Leong, S. W.; Mohd, S. M.; Abas, F.; Mohd Aluwi, M. F.; Rullah, K.; Lam, K. W.; Abdul Bahari, M. N.; Ahmad, S.; Tham, C. L.; Shaari, K.; Lajis, N. H.; Bioorg. Med. Chem. Lett. 2015, 25, 3330.

[23] Castellani, R. J.; Moreira, P. I.; Liu, G.; Dobson, J.; Perry, G.; Smith, M. A. Neurochem. Res. 2007, 32, 1640.

[24] Huang, X. Mutat. Res. 2003, 533, 153.

[25] Perron, N. R.; Brumaghim, J. L. Cell Biochem. Biophys. 2009, 53, 75.

[26] Yoshino, M.; Murakami, K. Anal. Biochem. 1998, 257, 40.

[27] Chorvant, R. J. Bioorg. Med. Chem. 2013, 23, 4751.

[28] a) Cerón-Romero, L.; Paoli, P.; Camici, G.; Flores-Morales, V.; Rios, M, Y.; Ramírez-Espinosa, J. J.; Hidalgo-Figueroa, S.; Navarrete-Vázquez, G.; Estrada-Soto, S. Bioorg Med Chem Lett. 2016, 26, 2018. b) Navarrete-Vázquez, G.; Morales-Vilchis, M. G.; Estrada-Soto, S.; Ramírez-Espinosa, J. J.; Hidalgo-Figueroa, S.; Nava-Zuazo, C.; Tlahuext, H.; Leon-Rivera, I.; Medina-Franco, J. L.; López-Vallejo, F.; Webster, S. P.; Binnie, M.; Ortiz-Andrade, R.; Moreno-Diaz, H. Eur J Med Chem. 2014, 3, 179.

[29] Ortiz-Andrade, R.; Navarrete-Vázquez, G.; Webster, S. P.; Binnie, M.; García-Jiménez, S.; León-Rivera, I.; Cigarroa-Vázquez, P.; Estrada-Soto, S. Diabetes Obes Metab. 2008, 10, 1097.

[30] Warne, X. T.; Edwards, P. C.; Leslie, A. G.; Tate, G. C. Structure 2012, 20, 841.

[31] (a) Biasini, M.; Bienert, S.; Waterhouse, A.; Arnold, K.; Struder, G.; Schmidt, T.; Kiefer, F.; Casarino, T.; Bertoni, M.; Bordoli, L. Nucleic Acids Res. 2014. 42, W252; (b). Arnold, K.; Bordoli, L.; Kopp, J.; Schwede, T. Bioinformatics 2006, 22, 195; (c) Kiefer, F.; Arnold, K.; Künzli, M.; Bordoli, L.; Schwede, T. Nucleic Acids Res.2009, 37, D387.

[32] Ortega-Gutierrez, S.; Lopez-Rodriguez, M. L. Mini Rev. Med. Chem. 2005, 5, 651.

[33] Cichero, E.; Menozzi, G.; Spallarossa, A.; Mosti, L.; Fossa, P. J Mol. Model. 2008, 14, 1131.

[34] Hollander, P. A.; Amod, A.; Litwak, L. E.; Chaudhari, U. Diabetes Care.2010, 33, 605.

[35] (a) Stierand, K.; Rarey, M. Med. Chem. Lett. 2010, 1, 540; (b) Stierand, K.; Rarey, M.; ChemMedChem. 2007, 2, 853; (c) Fricker, P.; Gastreich, M.; Rarey, M. J. Chem. Inf. Comp. Sci. 2004, 44, 1065.

[36] Sreejayan, N.; Rao, M. N. Arzneimittelforschung 1996, 46, 169.

[37] Benzie, I. F.; Strain, J. S. Anal. Biochem. 1996, 239, 70.

[38] Ramírez-Espinosa, J. J.; Rios, M. Y.; López-Martínez, S.; López-Vallejo, F.; Medina-Franco, J. L.; Paoli, P.; Camici, G.; Navarrete-Vázquez, G.; Estrada-Soto, S. Eur. J. Med. Chem. 2011, 46, 2243.

Legends

Table 1. Structures and DPPH scavenging of *N*'-arylidenehydrazones synthesized in this work

Table 2. ΔG_{bind} of hydrazones **3a**–**3j** and rimonabant.

Scheme and figures captions

Scheme 1. Synthesis of compounds **3a**–**3j**. Reactions and conditions: (a) LiHMDS, diethyl oxalate, MCH, r.t., 17 h; (b) 3,4-dichlorophenyl hydrazine, EtOH, H_2SO_4, reflux, 8 h; (c) KOH, EtOH, 50 °C, 12 h; (d) $SOCl_2$, PhMe, reflux, 2 h; (e) *tert*-butyl carbazate, DIPEA, $CHCl_3$, 0 °C to r.t., 4 h; (f) TFA, then vanillin, $AcOH_{cat}$, $CHCl_3$, r.t.

Figure 1. Structures of the pyrazole derivative rimonabant (**1**) and the hybrid **2**

Figure 2. Optimization of compound **2**. R^1 corresponds to different hydroxylated patterns.

Figure 3. Schematization of several antioxidant mechanisms that might be attributed to *N´*-acylhydrazones **3a**–**3j**. The figure shows the most active compound **3g**.

Figure 4. Antioxidant capacity of hydrazones **3a**–**3j** in FRAP test. Results are expressed as trolox equivalents (μmol trolox/g compound) ± SEM (n = 4)

Figure 5. Effect of a single dose of hydrazones **3a**–**3e** (A) and **3f**–**3j** (B) in a streptozotocin/nicotinamide rat model of diabetes (50 mg/kg; intragastric, n = 5). *p < 0.05; **p < 0.01; ***p < 0.001.

Figure 6. Predicted poses of hydrazones **3a**–**3j** inside the binding pocket of CB1R. Dashed lines illustrate hydrogen bonds between the carbonyl group and Lys192

Figure 7. Two-dimensional complex diagrams of the binding pose of **1** (A) and compound **3g** (B) inside the binding pocket of CB1R.

Graphical Abstract

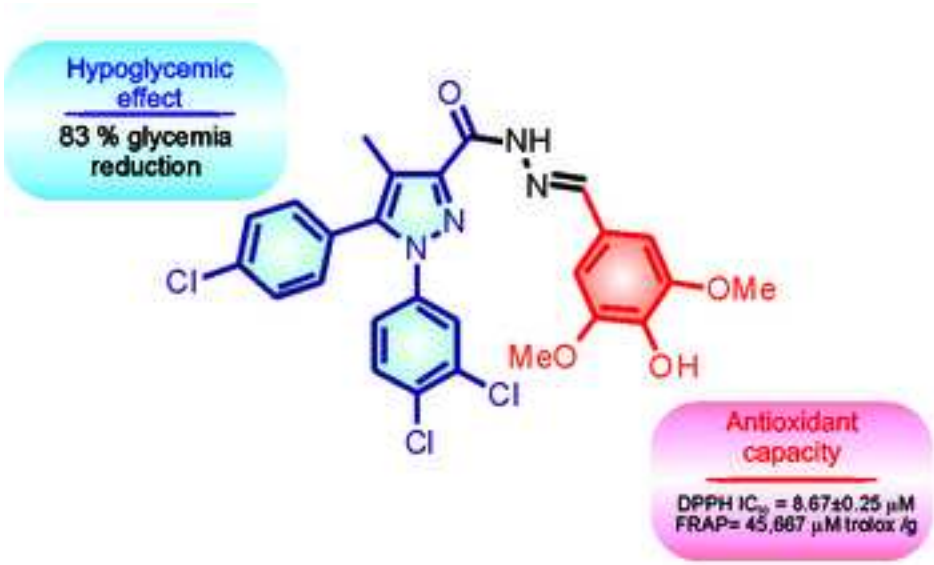

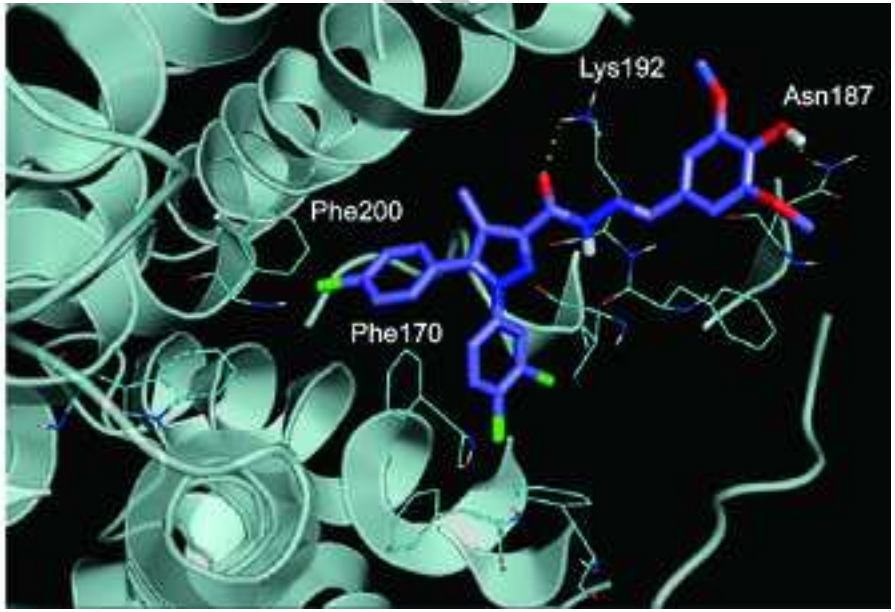

Highlights

Ten pyrazole-based hybrids were synthesized as hypoglycemic and antioxidant entities

Compounds bearing a 4-hydroxy group showed antioxidant activity in DPPH and FRAP assays

Analogues **3f** and **3g** had a glycemia reduction in an *in vivo* model of 83 and 90 %, respectively

Molecular docking demonstrated that compounds could reduce glucose by blockade of CB1R